ELSEVIER

Earth and Planetary Science Letters 206 (2003) 237–251

EPSL Frontiers

www.elsevier.com/locate/epsl

Frontiers

Strengthening the link between geochronology, textures and petrology

Wolfgang Müller *

Research School of Earth Sciences, Australian National University, Canberra, ACT 0200, Australia

Received 18 March 2002; received in revised form 25 September 2002; accepted 3 October 2002

Abstract

Time must be integrated with other geologic parameters such as pressure–temperature (*P-T*), composition or structural–textural information in order to quantify the dynamics of geologic processes like mountain building, faulting, metamorphism or magmatism. In the past, this connection was weak due to large sample sizes required in geochronology; however, recent developments open up exciting new possibilities. Texturally controlled in situ dating of minerals utilizing UV–laser ablation $^{40}Ar/^{39}Ar$ or Rb–Sr microsampling facilitates the crucial link between ages and textures at high spatial resolution. In situ U–Pb ages of accessory minerals can now be linked to the corresponding *P-T* evolution via their characteristic trace elemental signatures, indicative of mineral reactions in rocks. Garnet dating by Sm–Nd, and more recently Lu–Hf, can greatly benefit from both laser ablation inductively coupled plasma mass spectrometry (ICPMS) screening and improved leaching strategies, improving the link between time and *P-T*. Such integrated approaches can yield the duration and rates of deformation in shear zones, the rates of burial and exhumation of subducted rocks or the duration of entire metamorphic loops, to name a few. Potential for further development is identified in diverse areas. Dating of carbonate minerals related to brittle faulting using U–Pb could provide previously unavailable constraints on rates and duration of brittle deformation in the Earth's upper crust. In situ Rb–Sr dating applicable to micas could become available using either laser ablation dynamic reaction cell-ICPMS or microbeam accelerator mass spectrometry. Other future developments and trends, and their limitations, are discussed briefly.

Keywords: geochronology; petrology; structural geology; textures; rates; duration; P-T-t paths; Ar-40/Ar-39; Rb/Sr; Sm/Nd; U–Th–Pb; Lu–Hf; garnet; mylonites; dates; deformation; fault zones; laser ablation

1. Introduction

The field of linking geochronology to textures and petrology has seen rapid and unprecedented expansion during the last few years due to both development of various microbeam techniques and improvements in conventional techniques. Notably, the introduction of laser ablation systems has enabled in situ chemical analyses of trace elements and dating, particularly in the field of $^{40}Ar/^{39}Ar$ geochronology. This progress has resulted in several integrated geochronological studies, yielding rates and durations of geological pro-

* Tel.: +61-2-6125-9968; Fax: +61-2-6125-0738.
E-mail address: wolfgang.mueller@anu.edu.au (W. Müller).

0012-821X/02/$ – see front matter
doi:10.1016/S0012-821X(02)01007-5

Box 1
Definitions of acronyms and general information about techniques used in geochronology

Acronym	Explanation	Characteristics	Relevant key applications
TIMS	Thermal Ionisation Mass Spectrometry	Ions are formed in vacuum by heating a sample loaded onto a filament; applied to elements with relatively low first ionisation potential (e.g. Sr, Pb, Nd); various filament loading techniques are essential. Modern TIMS are equipped with multi-collector Faraday detection systems for simultaneous collection of several (≤9) isotopes (ion currents $>10^{-13}$ A), and single secondary electron multiplier (SEM) detectors for ion currents $\geq 10^{-18}$ A.	Most sensitive, high-precision technique for very small samples of certain elements (e.g. Sr, Pb) ; e.g. sub-ng Sr samples in case of Rb-Sr microsampling; few pg Pb for single mineral U-Th-Pb dating
ICP-MS	Inductively Coupled Plasma Mass Spectrometry (with quadrupole or sector-field mass analyser)	Ions are formed in an Ar plasma; especially useful for elements with high first ionisation potential (e.g. Hf, Th, W, Zn, Zr); Samples are introduced by solution nebulization; Large dynamic range single collector detection system	Rapid detection of relative concentrations; low precision isotope ratio analyses (>~1 ‰)
MC-ICPMS	Multi-Collector Inductively Coupled Plasma Mass Spectrometry	Sector-field ICPMS with multiple Faraday cup + SEM detection system similar to modern TIMS; ions are generated in a plasma (similar to above)	High-precision isotopic analyses of 'difficult' elements with high first ionisation potential (e.g. Hf, W, Th, Zn, Zr)
LA-ICPMS	Laser-Ablation ICPMS	Samples are introduced as a dry aerosol into an Ar plasma, after being ablated in a carrier gas (Ar, He) with a high power laser; used together with both ICPMS and MC-ICPMS	In-situ concentration and isotopic analyses
DRC	Dynamic Reaction Cell	Used in conjuction with ICPMS. Suppression of molecular interferences by reaction of the sample ions with a reactive gas (e.g. H_2, NH_3, CH_4, O_2, CH_3F, noble gases)	Elimination of Ar-based interferences (argides), selective conversion of atomic ions (e.g. Sr^+) to molecular ions (e.g. SrF^+)
SIMS	Secondary Ion Mass Spectrometry	Primary beam (e.g. Cs, O) sputters molecules and atoms off the sample; some are ionized during sputtering, extracted and analysed in a single collector detection system. Lower ablation rate than LA-ICPMS.	
SHRIMP	Sensitive High Resolution Ion Microprobe		In-situ U-Pb dating of U-rich accessory minerals
AMS	Accelerator Mass Spectrometry	Secondary negative ions are formed with a primary Cs ion beam; molecular ions are broken up at high energy levels in a tandem accelerator, thereby eliminating molecular interferences	Analysis of very low abundance isotopes (^{14}C); Selective use of molecular ions (e.g. SrH^-) to suppress isobaric interferences (e.g. for Rb-Sr)

cesses, rather than more conventional single time snapshots. This paper aims to highlight those innovations and tries to identify research areas where progress in the near future is likely to be made, or is desirable.

Time is a fundamental parameter in geology. The comparison between past and present as well as the evolution with time are key features of the Earth Sciences. Time, however, has to be linked with other parameters such as temperature, pressure, composition or structural–textural data in order to fully understand and quantify geological processes. Examples include dating of different stages of a pressure–temperature (*P-T*) loop in metamorphic terrains, the direct dating of ductile and brittle fault zones to constrain strain rates and duration of faulting, the dating of early diagenetic overgrowths in clastic sedimentary rocks, or determining the duration of magmatic events (Boxes 1, 2 and 3).

Establishing the link between ages, textures and *P-T* information has proven difficult in the past, mainly due to different sample sizes required by various techniques and the different scales at which they operate. Major element compositional data on the μm scale have been available since the early 1960s through electron microprobe analyses (EMPA), resulting in, for example, the derivation

Box 2
Overview of specific methods for linking geochronology with textures and petrology

Geo-chrono-meter	Method of operation	Key characteristics	Key examples of relevant applications	Selected referen-ces
$^{40}Ar/^{39}Ar$	UV-Laser-ablation	High spatial resolution; also ablates transparent minerals (e.g. white mica, feldspars)	In-situ dating of metamorphic white mica, depth profiling	[10]
			Dating of diagenetic K-feldspar overgrowths in clastic sediments	[16]
	Stepwise-heating	Discriminates between mineral phases via differential in-vacuo thermal breakdown	Dating of pseudotachylytes, or zoned amphiboles	[23, 24]
Rb-Sr	Microsampling + TIMS	Texturally-controlled extraction of minerals and subsequent conventional TIMS analysis	Dating of deformation; +dura-tion and rates; reliable dating of polymetamorphic rocks	[7, 38, 39]
	(LA-) DRC-ICP-MS	Elimination of isobaric interference at mass 87 by analyzing Sr as SrF^+ ions (no RbF^+ ions formed)	In-situ Rb/Sr dating of high Rb/Sr phases (micas) (?)	[42]
	Microbeam AMS ("AUSTRALIS")	Elimination of isobaric interference at mass 87 by selective formation of secondary SrH^- (but no RbH^-) ions with primary Cs^+ ions	In-situ Rb/Sr dating of high Rb/Sr phases (micas) (?)	[41, 84]
Sm-Nd, Lu-Hf	Conv. mineral se-paration + TIMS (Sm-Nd); + MC-ICPMS (Lu-Hf)	Garnet dating provides a key link between time and P-T; core – rim analyses to establish rates of garnet growth, burial and exhumation	Dating different stages of a metamorphic p-T loop;	[4, 53]
			Dating of eclogites	[51]
	LA-ICPMS	In-situ analyses of Sm-Nd abundances	Evaluation of effect of inclu-sions on garnet REE / Hf budget	[52]
U-Pb	Ion-microprobe (e.g. SHRIMP), LA-ICPMS	In-situ U-Th-Pb dating of e.g. zircon, monazite, titanite	Dating of magma crystallization or high-temperature metamorphism	[3, 72]
	Combined LA-ICP-MS / EMPA trace element analysis + SHRIMP dating	In-situ U-Th-Pb dating of accessory minerals (monazite, zircon, titanite) + link to P-T via trace elemental patterns (REE, Y) indicative of mineral reactions	Dating of different stages of a P-T loop, hence calibrating P-T-t paths	[60, 71]
	TIMS	High-precision single accessory mineral dating (and their fragments)	Dating of magma crystallization or high-T metamorphism	[75, 76]
	TIMS	U-Pb dating of carbonate minerals	Dating of tectonic carbonates (?)	[79, 88]

(?) indicates not yet available.

of *P-T* histories of rocks. In contrast, routine mineral dating until the mid-1990s usually required mg-sized mineral concentrates that could only be obtained by crushing of rocks and subsequent purification, with the inevitable loss of textural information. This bulk approach can also yield inaccurate ages by averaging mixtures of different generations of minerals preserving different ages, or by regressing minerals lacking isotopic equilibration. Conventional geochronological data were often only related to the (inferred) thermal evolution of the investigated area using the closure temperature concept, resulting in temperature–time paths, rather than integrating time into the full context of geological parameters. Notable early exceptions for the K–Ar and Rb–Sr systems [1,2] demonstrated that the careful application of standard techniques was capable of integrating geochronological results into a structural context, or provided a technique for dating of μg-sized samples. However, such methods were not widely applied until the mid-1990s.

In situ U–Pb dating of U-rich accessory phases is possible using the sensitive high-resolution ion microprobe (SHRIMP) developed at the Australian National University in the early 1980s [3], with spatial resolution (≤ 30 μm) approaching that attainable by EMPA. While this instrument had an enormous impact in Earth Sciences in general, linking ion microprobe U–Pb ages to the *P-T* evolution of metamorphic terrains initially was hampered because the conditions of formation

of minerals such as zircon, allanite or monazite can rarely be accurately determined (see below). From the 1980s onwards, Sm–Nd dating of garnets has provided another direct link between time and *P-T*, as detailed *P-T* conditions can be calculated for mineral reactions involving garnet. Dating cores and rims of large single garnets constrain duration and rates of metamorphism [4,5] (see below).

2. Present status of texturally controlled geochronology techniques

Several geochronometers allow time to be linked with other geologic parameters. They include the $^{40}Ar/^{39}Ar$, Rb–Sr, Sm–Nd, Lu–Hf, and U–Th–Pb dating techniques and their various modifications (see Boxes 1 and 2 for details). These methods enable either the dating of fabric-forming minerals, such as micas under full textural control (e.g. UV–laser ablation $^{40}Ar/^{39}Ar$, Rb–Sr microsampling), or the dated minerals can be linked to a *P-T* evolution using geothermobarometers or trace elemental patterns indicative of mineral growth (e.g. Sm–Nd, Lu–Hf, U–Th–Pb). The best targets, however, include minerals that unequivocally grew in response to deformation or metamorphism at temperatures below their respective isotopic closure, for example syndeformationally grown fibres between stretched porphyroclasts in mylonites ([6,7]; Fig. 1). Detailed imaging prior to (in situ) dating by optical microscopy, backscattered-electron secondary-electron-microscopy (BSE-SEM), or orientation contrast is of prime importance to reveal phase relationships, homogeneity of minerals, the presence of multiple generations etc.

2.1. $^{40}Ar/^{39}Ar$ method

$^{40}Ar/^{39}Ar$ is a variant of K–Ar dating and is based on the decay of ^{40}K to ^{40}Ar (half-life: 1.25 Ga). Potassium is a major element in micas or K–feldspars, whereas Ar is usually a rare and highly incompatible trace element. This makes K–Ar a very sensitive chronometer covering the entire geological time scale (10^3–10^9 a). Conventional K–Ar requires separate analyses of K and Ar on different instruments and sample aliquots, which, in practical terms, makes it cumbersome and prone to sample inhomogeneities. Neutron activation of K-bearing samples, however, produces ^{39}Ar from ^{39}K and overcomes the limitations

Box 3
Terminology related to structures, textures and petrology

Term	Explanation
Texture, structure, fabric	Spatial and geometrical configuration and the mutual relationships of all components making up a rock; fabric elements should be more or less penetratively developed throughout a rock; texture often refers to small-scale, structure to large-scale features
Foliation	Planar arrangement of textural or structural features in rocks, especially in metamorphic rocks
Mylonite	Foliated and lineated fault rock showing features indicative of strong ductile deformation (mylonite zones are interpreted as 'fossil' ductile shear zones)
Pseudotachylyte	Very fine-grained to (rarely) glassy veins associated with faults or meteorite impacts that show sharp, intrusive contacts to the host rock. Inclusions of minerals (usually only quartz and feldspar) and wall rock fragments are common. P. is thought to represent products of ancient frictional melting.
Fault gouge	Fine-grained, incohesive fault rock associated with shallow brittle fault zones (cataclasis), often with clay minerals as matrix
Slickenside	Discrete, sometimes polished fault surface associated with brittle deformation, often with striations and (slicken)fibres grown in response to fault movement (Fig. 4b)
Strain fringe	Syn-deformational mineral fibres grown in response to strain perturbations (strain shadow) adjacent to rigid objects in shear zones (Fig. 1b)
Mica, phengite	K-rich phyllosilicate, either Al-rich (white mica) or (Mg-Fe)-rich (biotite); Phengites are high-pressure modifications of white mica, with some (Mg, Fe) entering the Al position, coupled with a corresponding increase of Si to maintain the charge balance
D1, D2, D3, S1…	Common terminology used in structural geology to denote the relative sequence of deformations (D) and/or foliations (S)
P-T-t	Pressure-Temperature-time

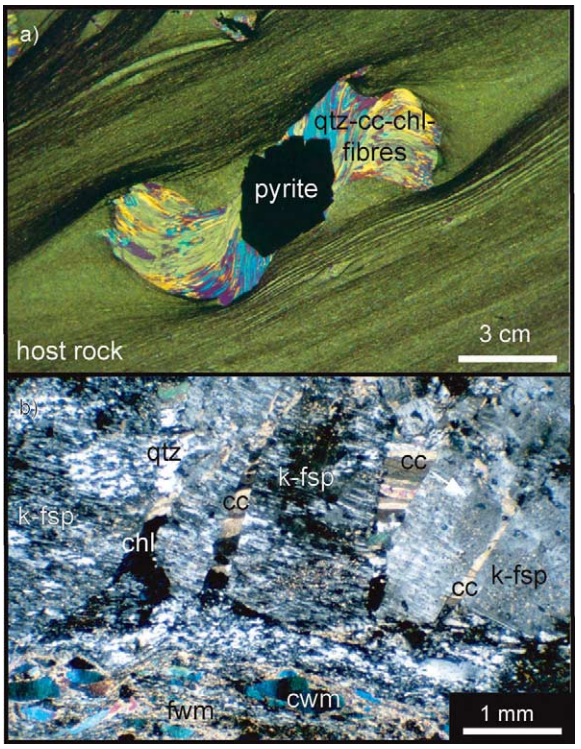

Fig. 1. Examples of strictly syndeformationally grown minerals in shear zones. (a) Quartz–calcite–chlorite fibres (qtz–cc–chl) grown antitaxially in the strain shadow of a large pyrite in response to deformation (mylonitized slate, Lourdes, N. Pyrenees [82]). These fibres record two distinct stages of deformation related to the northward thrusting of the external Pyrenees. Rb–Sr microsampling dating of four successive increments of fibre growth constrains both duration and rates of faulting; chlorite+quartz have elevated Rb/Sr ratios, whereas cogenetic calcite constrains the initial Sr isotopic composition [7]. (b) Calcite–quartz–chlorite fibres (cc–qtz–chl) grown between stretched K–feldspar (k–fsp) porphyroclasts in a greenschist facies basement mylonite (W DAV fault, Eastern Alps [39]). This is a key example illustrating the importance of texturally controlled microsampling dating: for the most reliable dating of deformation, newly grown fibres such as the ones between stretched K–feldspar porphyroclasts are to be used rather than coarse (cwm) or fine-grained (fwm) white mica in the matrix of the mylonite.

of K–Ar, by enabling the measurement of both parent and daughter elements in one single Ar isotopic analysis. The resulting $^{40}Ar/^{39}Ar$ method is simpler and more powerful than conventional K–Ar (for a review see [8]). Argon for $^{40}Ar/^{39}Ar$ analysis can be released from minerals in several ways, with stepwise heating in a furnace and laser extraction being the most common.

The obvious advantage in extracting Ar with a laser is the ability to perform in situ analyses. Although laser-based Ar extraction has been applied to extraterrestrial samples since the early 1970s and to terrestrial rocks since the early 1980s (for a review see [9]), only the advent of ultraviolet (UV)–laser ablation facilitated analyses with the required high spatial resolution, thus making $^{40}Ar/^{39}Ar$ dating a microprobe technique. Minerals absorb laser energy better at shorter wavelengths [10], facilitating the UV–laser ablation of transparent minerals such as white mica, feldspars or quartz, which are otherwise poor absorbers of higher wavelength lasers. UV–laser ablation has a spatial resolution of ≤ 10 μm and a depth resolution of ~ 1 μm [10].

Key applications of UV–laser ablation $^{40}Ar/^{39}Ar$ dating include dating of deformation [11], the study of intragrain argon transport processes in minerals [12,13], dating of impact-related pseudotachylytes [14], dating of different stages of one *P-T* loop [15], dating of K–feldspar cements [16], establishing the speed of kimberlite ascent [17], studying magma flow regimes in sills from Ar systematics in host rock micas [18], dating of mineral inclusions in porphyroblasts [19] amongst others.

During stepwise heating $^{40}Ar/^{39}Ar$ analysis, Ar is sequentially released from the sample by increasing the temperature of a vacuum furnace and analysing the Ar isotopic composition of each step. Stepwise gas release can also be achieved with a defocused laser beam. In the beginning of $^{40}Ar/^{39}Ar$ work, stepwise Ar release was considered to primarily reveal information about the spatial distribution of Ar within a mineral [8]. However, more recent work has demonstrated that especially hydrous phases (micas, amphiboles) are unstable during in vacuo heating and yield only limited, if any, information about the intragrain Ar distribution [20–22]. On the other hand, compositionally heterogeneous minerals or multiphase samples have been shown to release Ar over characteristic stages during a step-heating experiment [23,24]. Using the direct compositional information from ^{37}Ar, ^{38}Ar and ^{39}Ar produced

by neutron reactions from Ca, Cl and K, respectively, individual steps can be related to certain minerals present in chemically non-uniform samples [23–25]. Crucial for this successful link is EMPA data that can be compared with Ca/K and Cl/K ratios calculated from $^{40}Ar/^{39}Ar$ analyses. The theoretical spatial resolution of differential Ar release by step heating is controlled by the reactor-induced recoil redistribution of Ar isotopes, i.e. $< \sim 0.5$ μm [26]. Using this indirect method for linking time, composition and textures, zoned amphiboles or pseudotachylytes, for example, can be reliably dated [23,24]. This contrasts in situ laser ablation $^{40}Ar/^{39}Ar$ analysis, which in the presence of inhomogeneities on the ~ 10 μm scale may yield inaccurate ages due to mixing of unrelated components, such as very fine-grained inherited clasts present in a pseudotachylyte matrix [24].

Dating of clays is crucial for the geochronology of brittle faults (fault gouges) or sediments. Fine-grained minerals such as clays (< 2 μm) pose difficulties for $^{40}Ar/^{39}Ar$ dating, due to the recoil-induced redistribution and subsequent loss of reactor-produced ^{39}Ar and ^{37}Ar [26]. Vacuum encapsulation allows monitoring of ^{39}Ar loss from thin clay minerals and enables $^{40}Ar/^{39}Ar$ dating of μg-sized clay samples [27,28]. In addition to the dating difficulty, clay samples consist of mixtures between differently aged authigenic and detrital components, which have to be resolved in order to arrive at accurate ages. Two techniques have recently been proposed to overcome the problem. Ages of both clay 'endmember' components can be determined due to differences in thermally activated Ar release between authigenic and detrital clay minerals, as revealed by laser-stepped heating [27]. Dating combined with detailed XRD analysis of several grain size fractions of clays in fault gouges allows for the extrapolation of ages of clay mixtures to both pure authigenic and pure detrital 'endmember' ages [29]. Whether these techniques are applicable if more than two generations of clay minerals are present, remains to be tested, but they offer exciting possibilities for the difficult dating of fault gouges and our understanding of brittle faults. In situ $^{40}Ar/^{39}Ar$ dating of clays was proposed by [30] applying their retention age concept [31], but the capability of this technique to separate differently aged components within a clay sample has yet to be explored.

Excess ^{40}Ar (see [32] for a review), a known complicating factor for $^{40}Ar/^{39}Ar$ dating of high-pressure rocks [33] or deformation [24,34], is sometimes difficult to detect unless multi-chronometric approaches are utilized [35]. UV–laser ablation $^{40}Ar/^{39}Ar$ profiling of individual minerals allows the detection of intragrain ^{40}Ar gradients, and hence may reveal excess ^{40}Ar contamination [12]. Combined Rb–Sr microsampling and UV–laser ablation $^{40}Ar/^{39}Ar$ dating of minerals grown in a strain fringe around pyrite from the Eastern Alps (Fig. 2) [36] have revealed excess ^{40}Ar (Müller and Wartho, unpublished data). This locality appears to record deformation-induced fibre growth at ~ 32–40 Ma according to Rb–Sr microsampling ages. However, UV–laser ablation $^{40}Ar/^{39}Ar$ analyses have yielded high and variable amounts of ^{40}Ar but virtually no ^{36}Ar, with apparent ages of white mica ranging between 97 and 370 Ma. This demonstrates again the need for caution when interpreting apparent $^{40}Ar/^{39}Ar$ ages in deformed rocks.

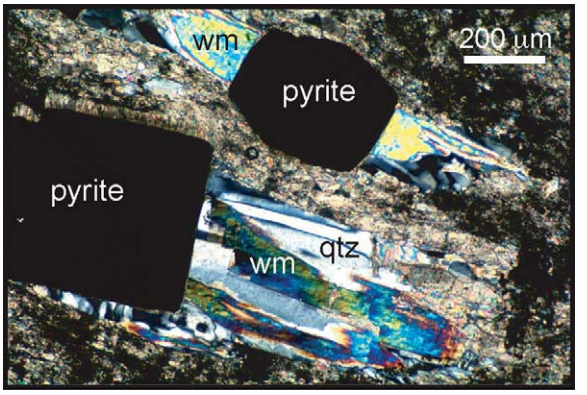

Fig. 2. Strain fringes around pyrite in a deformed slate, containing rare, large, newly grown white mica (wm) together with quartz (qtz) and calcite (not shown) (Eastern Alps [36]). Preliminary, combined Rb–Sr microsampling and UV–laser ablation $^{40}Ar/^{39}Ar$ dating revealed large amounts of excess ^{40}Ar, a common situation in deformed rocks, making reliable $^{40}Ar/^{39}Ar$ dating of mylonites difficult.

2.2. Rb–Sr microsampling dating

The decay of ^{87}Rb to ^{87}Sr (half-life: 48.8 Ga) can be utilized for dating of Rb-bearing minerals such as micas, as Rb geochemically resembles K. This geochronometer was initially investigated by [37] and continuously improved both with respect to precision and sample size (e.g. [2,38,39]). Modern multi-collector thermal ionization mass spectrometers (TIMS), combined with careful filament loading techniques [40], are characterized by Sr ionization efficiencies up to 5% and facilitate precise analyses of $\leq 10^{-9}$ g Sr [39]. Samples can be as small as a few μg, due to high concentrations of Rb and Sr in certain minerals (often ≥ 50 ppm in micas) and substantial parent–daughter elemental fractionation. Because of these technical improvements, minerals to be dated can be cut out of ~ 50 μm thick rock sections under full textural control using a microdrill mounted onto a microscope (Fig. 3) [39]. After documentation by optical or SEM imaging, microsampling, dissolution and ion-exchange chemistry, ng-sized Sr samples are analysed by TIMS, which requires Sr blank levels in the lower pg range [39]. Rb–Sr microsampling dating enables linking ages with the textural or *P-T* evolution of a sample, similar to in situ ^{40}Ar/^{39}Ar dating, but it also has some advantages. Rb–Sr microsampling dating is not affected by excess argon, makes the analysis of low-K minerals such as chlorite possible, and many minerals are characterized by higher closure temperatures for Rb–Sr when compared to K–Ar.

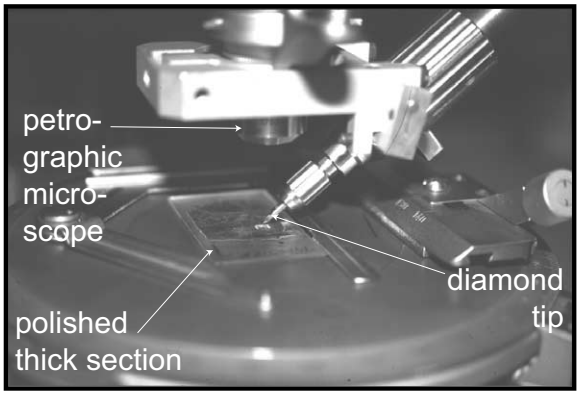

Fig. 3. Microdrill used for sample preparation for Rb–Sr microsampling [39]. The drill is mounted onto the lens of a conventional petrographic microscope and any desired shape of sample can be cut out of a rock thick section by moving the microscope stage relative to the rotating, tapered diamond tip. Heating and liquefying the glue helps extracting samples. A 400 μm square of white mica (Sr concentration of 50 ppm) excised from a 50 μm thick section contains ~ 1 ng Sr. Even smaller samples can be cut out of thicker sections; the limitation being the ability to observe through $\gg 50$ μm thick sections and the width of cuts (~ 50–100 μm) made by tapered diamond drills.

This time-consuming technique is necessary because the isobaric interference at mass 87 (β^- decay of ^{87}Rb to ^{87}Sr) requires complete separation of Rb and Sr before mass spectrometry. Even at highest mass resolution (10 000), current mass spectrometers are unable to separate ^{87}Rb and ^{87}Sr. This has so far prevented the implementation of an in situ Rb–Sr dating technique for minerals with high Rb/Sr ratios, such as micas in differentiated granites or pegmatites (and their deformed counterparts) with typical Rb/Sr ratios of > 100. For a successful in situ Rb–Sr dating technique, Rb and Sr thus have to be chemically separated on-line, or Sr has to be analysed as molecular species, which does not form Rb ions [41,42] (see Section 3). Strontium isotope ratios can also be analysed by in situ laser ablation multi-collector inductively coupled plasma mass spectrometry (MC-ICPMS) [43]. However, this is of limited use for dating purposes, as only samples with low Rb/Sr ratios (< 0.2) and high Sr concentrations, such as carbonates or feldspars, can be analysed [43,44]. This technique therefore is more important in Sr isotope geochemistry. When compared to MC-ICPMS, TIMS is still the more sensitive analytical technique for small samples ($\leq$ few ng Sr).

A key example of texturally controlled Rb–Sr microsampling is the dating of syndeformationally grown fibres (strain fringes, Fig. 1a) from a shear zone in the Pyrenees, with the aim of constraining both strain rates and the duration of shear zone activity [7]. This study yielded a long duration of shear zone activity of ~ 37 Myr (87–50 Ma), with a low average strain rate of 1.1×10^{-15} s^{-1}. During a ~ 4 Myr interval (66–62 Ma), the strain rate increased to 7.7×10^{-15} s^{-1}, which coincided with the change in fibre growth direction and the reorientation of the stress field to renewed horizontal

compression. Another example of Rb–Sr microsampling dating [45] illustrates the difficulties of establishing an accurate chronology in polymetamorphic basement gneisses from the Western Alps, where previous conventional Rb–Sr dating of mineral concentrates [46] had failed to yield a reliable age of metamorphism due to isotopic disequilibria. Different generations of coarse- and fine-grained white micas from both strongly and weakly foliated domains have been dated by Rb–Sr microsampling. There is evidence for isotopic disequilibrium among individual coarse white micas and feldspar even on the thin section scale, whereas fine-grained white micas and adjacent feldspar mosaic are in equilibrium and record Tertiary ages, exemplifying the necessity of texturally controlled dating.

2.3. Sm–Nd, Lu–Hf dating

The rare earth element (REE) isotopes ^{147}Sm and ^{176}Lu decay to ^{143}Nd and ^{176}Hf, respectively, with half-lives of 106 and 37.2 Ga [47,48]. Garnet is the main target of REE-based Sm–Nd and Lu–Hf dating, as its lattice preferentially incorporates heavy REE (HREE) and, therefore, shows elevated Sm/Nd and Lu/Hf ratios. Garnet as a major constituent of metamorphic and some magmatic rocks is also widely used in geothermobarometry, thus providing a direct link between *P-T* and time. Garnet has a high closure temperature in both the Sm–Nd and Lu–Hf systems (>650°C; e.g. [49,50]). However, low concentrations of REEs and Hf, the associated susceptibility of garnet to the presence of REE/Hf-rich inclusions (e.g. allanite, monazite, zircon) and the limited fractionation of mother and daughter elements, make Sm–Nd and Lu–Hf garnet dating analytically challenging. The recent advent of MC-ICPMS has facilitated the precise analysis of ng-sized quantities of Lu and Hf, opening up an avenue for Lu–Hf dating of garnet [49,51]. In order to evaluate the effect of mineral inclusions on TIMS Sm–Nd ages obtained on mg-sized garnet separates, TIMS Sm–Nd data have been compared with corresponding in situ Sm–Nd abundances determined by laser ablation [52]. These authors confirm that Sm/Nd ratios are generally negatively correlated with Nd concentration. However, they also report garnets with >5 ppm Nd and elevated Sm/Nd ratios (≤ 1.8), where the REEs are shown to reside in the garnet lattice and not in inclusions.

Direct constraints on the rates and duration of metamorphic processes have been derived from Sm–Nd and Rb–Sr dating of rims and cores of large garnets (e.g. [4,5,53]). Such studies yielded growth intervals of 3 and 32 Ma, growth rates between 0.2 and 2 mm Ma^{-1}, shear strain rates derived from garnet rotation of $2–3\times10^{-14}$ s^{-1}, as well as burial and heating rates. Some early applications of Sm–Nd garnet dating reported concordant U–Pb and/or Rb–Sr ages, which, however, need to be interpreted with care given the documented presence of both equilibrated and unequilibrated U- or Sr-bearing inclusions in garnet [54,55].

Sm–Nd, and increasingly, Lu–Hf analyses are used for dating of eclogites, which trace important subduction-related stages of the evolution of orogens and constrain the timing of continental collision. Eclogites derived from coarse-grained gabbroic precursors in particular, however, are often plagued by isotopic disequilibria between minerals, notably garnet and clinopyroxene, which makes reliable dating difficult [56,57]. Oxygen isotopes can help to elucidate whether the eclogite minerals used for dating are in isotopic equilibrium [58]. Lu–Hf dating of garnet is still in its infancy, but it is obvious that one of the limiting factors for its widespread application in crustal rocks will be the ubiquitous presence of (unequilibrated) zircon, both as inclusions in garnet and in the matrix, with Hf concentrations up to several % [49] (see Section 3).

2.4. U–Th–Pb dating

The decay of uranium (^{238}U, ^{235}U) and thorium (^{232}Th) to stable lead (^{206}Pb, ^{207}Pb, ^{208}Pb) is the basis for the most precise and versatile chronometers. Due to the high closure temperatures of U-rich accessory minerals such as zircon, monazite, xenotime, allanite or titanite, U–Th–Pb is mainly applied to the dating of magmatic rocks, high temperature stages of metamorphic rocks or old

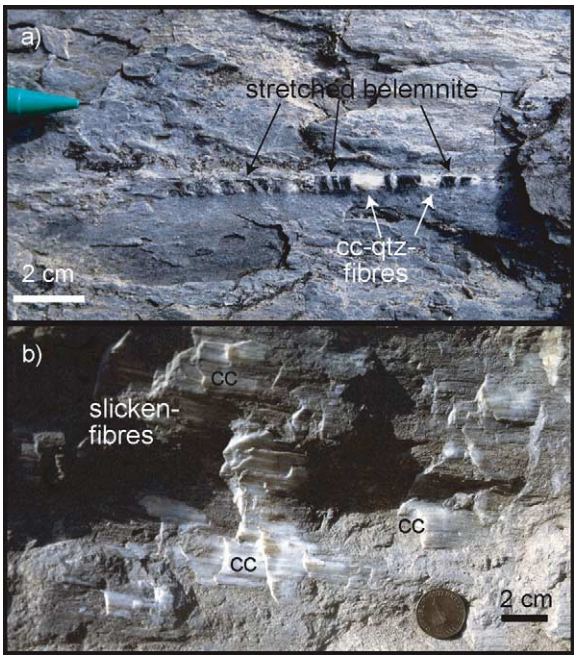

Fig. 4. Examples of tectonic carbonates. (a) Stretched belemnite in Liassic slates with intervening calcite–quartz (cc–qtz) fibres grown in response to deformation (Leytron, Helvetics, Central Alps [81]). (b) Calcite (cc) slickenfibres grown on slickensides in response to dextral brittle faulting of limestones, which are very common in brittly faulted limestone terrains (Gosau, Eastern Alps [86]). If datable by U–Pb, as preliminarily indicated by their elevated U–Pb ratios, such fibres would provide previously unavailable constraints on ages, duration and rates of brittle faulting.

detrital components in sedimentary rocks. Zircon especially may show growth zones recording multiple magmatic/metamorphic stages, the unraveling of which demands in situ dating using ion probes, such as SHRIMP [3].

Relating U–Th–Pb ages of accessory minerals to the *P-T* conditions in metamorphic rocks is difficult. In situ dating of monazite inclusions in large garnets, for example, [59,60] links monazite ages to the garnet *P-T* history, provided the two have formed in equilibrium at the same time. The Y-content of metamorphic monazite provides another link to mineral (garnet) growth in a rock and hence *P-T* conditions [60]. Ion microprobe Th–Pb depth profiling of individual monazites is capable of resolving age differences at the 0.05 μm scale, as a result of much better depth resolution when compared to spot size (~20 μm [61]). From coexisting and equilibrated monazite–xenotime pairs, both precise U–Th–Pb ages and temperatures can be derived due to the temperature-dependent exchange of REEs and Y between these minerals [62–64]. However, both monazite and xenotime appear to be sensitive to secondary alteration, such as low-temperature fluid interaction [65].

In order to extract time information about multiple tectonic events, mainly zircons have been in situ dated by ion microprobe (SHRIMP). Distinct domains (magmatic and/or metamorphic) present in single zircons that correspond to different tectonic events can be identified using cathodoluminescence or SEM imaging [66]. Following this approach, domains in zircons from early deformed veins, eclogites and crosscutting pegmatites, all interpreted to represent one subduction-related *P-T* cycle, have been dated [67]. The resulting rates of burial and exhumation approximated plate tectonic speeds. Similar conclusions have been drawn from SHRIMP U–Pb dating of different generations of titanite, a major constituent of many rocks, for which detailed *P-T* conditions had been established [68]. Mineral inclusions in zircon also provide invaluable clues for the calibration of a *P-T-t* path [69]. SHRIMP U–Pb dating combined with trace elemental data such as REE patterns from laser ablation ICPMS analyses allow zircon domain formation to be linked to mineral reactions taking place in the rock, and therefore relates zircon growth to the main paragenesis and *P-T-t* evolution of a rock [70,71].

In situ U–Pb dating using laser ablation ICPMS offers an alternative to ion microprobe-based U–Pb dating of accessory minerals [72,73]. LA-ICPMS U–Pb dating does not require an external calibration because of simultaneous nebulization of standard solutions to assess elemental and isotopic fractionations. When compared to ion microprobes, LA-ICPMS dating consumes more sample and suffers from elevated Hg backgrounds interfering at ^{204}Pb, but is more readily available and cheaper (see [74] for a more extensive discussion).

Conventional TIMS U–Th–Pb dating of single grains of accessory minerals (and fragments there-

of) achieves superior precision when compared to in situ dating by ion microprobes [75]. Comparative U–Pb and Th–Pb dating, especially of high Th/U minerals (allanite, monazite), can reveal the presence of initial disequilibrium signatures within the U–Pb decay chains, constraining of whether ages represent growth or cooling/resetting episodes (for a review, see [76]). Another technique for relating U–Th–Pb ages to structural/textural data is dating of variably deformed intrusions in relationship to fault zones or regional deformation events [77].

U–Pb dating of carbonates could provide another possibility for linking low-temperature structures and geochronology (Fig. 4). Calcite, aragonite and secondary carbonate cements often show elevated U/Pb ratios (e.g. [78,79]). U^{4+} has been shown to replace Ca^{2+} in the calcite lattice, confirming that U is not just concentrated in inclusions [80]. Carbonate veins or fibres are ubiquitous tectonic features in many deformed rocks used to reconstruct the strain history of an area [81]; however, no attempt has been made to directly date such structures (see Section 3).

3. Discussion and outlook

Establishing a reliable connection between geochronological ages and other geologic parameters (temperature, pressure, composition or structural–textural data) is difficult, yet increasingly possible using the recent methodological developments detailed above. Strengthening this integrated approach is essential for a further in-depth understanding of the dynamics of lithospheric processes, and will advance our insight into processes as diverse as mountain building, faulting, exhumation, or magmatism, to name a few. The ability to constrain the duration and calculate rates of geologic processes is arguably the most important outcome of this successful integration of different approaches, for example applied to the study of metamorphism [67,68] and fault zones [7].

Besides problems with geochronological techniques, there are inherent uncertainties with microstructural interpretations. For example, tectonic foliations are often reactivated during multiple deformation events, which is why 'foliation ages', e.g. conventional ages of fabric-forming micas, may not accurately yield the true age of fabric formation. A good example is given by fibrous strain fringes from the N. Pyrenees [7,82] (Fig. 1a). In these samples, the main foliation (referred to as S1) was reactivated during subsequent, strain fringe-forming deformations (D2 and D3). Dating those fibres reliably establishes both the duration of fibre growth (D2, D3) and the transition between the two, but only yields a minimum age for the formation of the main foliation (D1). Apart from microstructures, progress in the derivation of *P-T* conditions in rocks, as for example provided by the use of 'pseudosections' [83], and an improved understanding of intragrain transport processes of geochronologically important elements will help strengthening the connection between time and other geological variables. A more detailed discussion, however, is beyond the scope of this overview.

The following technical or conceptual developments are either currently underway or are desired in order to improve our understanding of the timescale of geologic processes. Progress is likely to happen in, but not restricted to:

- Rb–Sr dating: a direct 'on-line' elimination of the isobaric interference problem at mass 87 (^{87}Rb and ^{87}Sr) with the aim of in situ Rb–Sr dating of minerals with high Rb/Sr ratios (e.g. micas) would provide a breakthrough. Two ways of achieving this objective appear to be possible.

(a) Use of a dynamic reaction cell (DRC) in conjunction with a quadrupole-ICPMS, by which SrF^+ ions, but no RbF^+ ions are produced via reaction with CH_3F [42]. SrF^+ rather than Sr^+ is analysed, thus eliminating the Rb–Sr interference. Resultant $^{87}Sr/^{86}Sr$ ratios yield precisions at the sub-‰ level, and Rb/Sr ratios can be determined, too. It remains to be tested whether this technique is applicable to in situ laser ablation analysis. The dependence of mass bias and parent/daughter ratios on matrix composition must also be assessed.

(b) Use of microbeam AMS (accelerator mass spectrometer) with a primary Cs^+ beam (spatial resolution ≤ 30 μm), which produces negative

secondary ions. The selection of appropriate molecular species, such as SrH^- instead of Sr^-, eliminates the isobaric interference at mass 87, because RbH^- ions are not formed ([41]). Microbeam AMS has been shown to achieve sub-‰ precision for Pb isotopes [84], and is currently explored for in situ Re–Os dating of minerals with elevated Re/Os ratios, such as molybdenite. The obvious drawback of microbeam AMS is the greater cost of the system, and it is less readily available when compared to DRC-ICPMS. With respect to applications of in situ Rb–Sr dating, in particular white mica with its fairly high closure temperature ($\geq \sim 550$°C [38,85]) allows the derivation of growth ages rather than cooling ages for mica-forming reactions and deformation up to high greenschist facies metamorphic conditions.

- U–Pb dating of tectonic carbonates such as those occurring in veins or as newly grown fibres on brittle faults (slickensides [81], Fig. 4b) could provide essential, presently unavailable constraints on ages, rates and duration of low-temperature, semi-brittle deformational events. Preliminary trace elemental data for a ~ 5 mm thick, ~ 10 mm long calcite slickenfibre related to Miocene faulting in the Eastern Alps [86] (Fig. 4b) have been obtained using laser ablation ICPMS (for technical aspects of the LA-ICPMS system used, see [87]). U and Pb concentrations range between 25 and 200 ppb and 34 and 36 ppb, respectively; and corresponding $^{238}U/^{204}Pb$ (μ) ratios vary between 50 and 390 and compare well with U–Pb data from sedimentary or ore-stage calcites (e.g. [79,88]). However, it remains to be tested whether the U–Pb system of tectonic carbonates is resistant to secondary alteration, for example induced by later faulting or fluid flow.
- Evaluation of the possible preservation of isotopic (i.e. age) inheritance in compositional–structural relicts: Metamorphic rocks often contain relicts formed at different stages of one or more *P-T-t* path(s), which can be detected by EMPA or SEM imaging. Examples include phengite cores in white mica [89], compositionally complex amphiboles [23] or zoned garnets [90]. The preservation of petrographic relicts especially at low to intermediate metamorphic grades strongly suggests isotopic inheritance, since the rate-determining process for re-equilibration of trace elements important in geochronology (e.g., Sr, Ar) is controlled by the transport of major cations [85]. In situ $^{40}Ar/^{39}Ar$ dating of compositionally zoned white mica has indeed observed a correlation of older ages with structural–compositional relicts in gneisses hosting eclogites [15]. The authors suggest that these micas record $^{40}Ar/^{39}Ar$ ages at temperatures ≥ 550°C, similar to conclusions drawn by [91]. More work is required to assess the equilibration of isotopic systems in compositional relicts of polymetamorphic rocks, and it could also be extended to the Rb–Sr system of white mica, either by conventional microsampling [39] or true in situ Rb–Sr dating, as outlined above.
- New ways for improved Sm–Nd and Lu–Hf dating of garnet: screening of garnet prior to mineral separation using LA-ICPMS will yield direct information on Sm–Nd and Lu–Hf ratios, their respective concentrations and the presence of inclusions. Routine leaching of crushed garnet separates with 'new' leaching agents such as sulphuric acid will enhance both precision and accuracy of Sm–Nd and Lu–Hf dating [92,93]. An assessment of a dissolution strategy for Lu–Hf dating of garnet without attacking Hf-bearing zircon inclusions is desirable (cf. [55]), e.g. with concomitant monitoring of Zr release.
- Improving the technique of combined in situ U–Th–Pb dating and LA-ICPMS (REE) or EMPA (Y) trace elemental analysis of accessory minerals. This will place better constraints on the formation of dated minerals in the context of mineral reactions, and hence *P-T* conditions in rocks [60,71].

Acknowledgements

Supported by a Swiss National Science Fund postdoctoral fellowship. An earlier version of this paper was considerably improved by D. Aerden, R. Anczkiewicz, J.P. Bernal, E. Calvo, D. Durney, T. Esat, C. Pelejero, D. Rubatto, and J.-A. Wartho, which is gratefully acknowledged. Reviews by Derek Vance and two anonymous

referees significantly helped to clarify many aspects of this paper. Thanks to Alex Halliday for providing the incentive to write this paper. *[AH]*

References

[1] R.H. Steiger, Dating of orogenic phases in the Central Alps by K-Ar ages of hornblende, J. Geophys. Res. 69 (1964) 5407–5421.
[2] D.A. Papanastassiou, G.J. Wasserburg, Microchrons: the 87Rb-87Sr dating of microscopic samples, Proc. Lun. Planet. Sci. Conf. 12B (1981) 1027–1038.
[3] W. Compston, I.S. Williams, C.E. Meyer, U-Pb geochronology of zircons from lunar breccia 73217 using a sensitive high mass-resolution ion microprobe, in: Proceedings of the Fourteenth Lunar and Planetary Science Conference, Part 2, J. Geophys. Res. B 89 Suppl. (1984) 525–534.
[4] K.W. Burton, R.K. O'Nions, High-resolution garnet chronometry and the rates of metamorphic processes, Earth Planet. Sci. Lett. 107 (1991) 649–671.
[5] J.N. Christensen, J.L. Rosenfeld, D.J. DePaolo, Rates of tectonometamorphic processes from rubidium and strontium isotopes in garnet, Science 244 (1989) 1465–1469.
[6] W.J. Dunlap, C. Teyssier, I. McDougall, S. Baldwin, Ages of deformation from K/Ar and Ar-40/Ar-39 dating of white micas, Geology 19 (1991) 1213–1216.
[7] W. Müller, D. Aerden, A.N. Halliday, Isotopic dating of strain fringe increments: duration and rates of deformation in shear zones, Science 288 (2000) 2195–2198.
[8] I. McDougall, T.M. Harrison, Geochronology and Thermochronology by the 40Ar/39Ar Method, xii, Oxford University Press, New York, 1999, 269 pp.
[9] S.P. Kelley, Ar-Ar dating by laser microprobe, in: P.J. Potts, J.F.W. Bowles, S.J.B. Reed, M.R. Cave (Eds.), Microprobe Techniques in the Earth Sciences, Mineralogical Society Series 6, Chapman and Hall, London, 1995, pp. 123–143.
[10] S.P. Kelley, N.O. Arnaud, S.P. Turner, High spatial resolution Ar-40 Ar-39 investigations using an ultra-violet laser probe extraction technique, Geochim. Cosmochim. Acta 58 (1994) 3519–3525.
[11] A. Mulch, M.A. Cosca, M.R. Handy, In-situ UV-laser 40Ar/39Ar geochronology of a micaceous mylonite: an example of defect-enhanced argon loss, Contrib. Mineral. Petrol. 142 (2002) 738–752.
[12] S.M. Reddy, S.P. Kelley, J. Wheeler, A Ar-40/Ar-39 laser probe study of micas from the Sesia Zone, Italian Alps: implications for metamorphic and deformation histories, J. Metamorph. Geol. 14 (1996) 493–508.
[13] J.A. Wartho, S.P. Kelley, R.A. Brooker, M.R. Carroll, I.M. Villa, M.R. Lee, Direct measurement of Ar diffusion profiles in a gem-quality Madagascar K-feldspar using the ultra-violet laser ablation microprobe (UVLAMP), Earth Planet. Sci. Lett. 170 (1999) 141–153.
[14] J.G. Spray, S.P. Kelley, W.U. Reimold, Laser probe Ar-40 Ar-39 dating of coesite-bearing and stishovite-bearing pseudotachylytes and the age of the Vredefort impact event, Meteoritics 30 (1995) 335–343.
[15] G. DiVincenzo, B. Ghiribelli, G. Giorgetti, R. Palmeri, Evidence of a close link between petrology and isotope records: constraints from SEM, EMP, TEM and in situ Ar-40-Ar-39 laser analyses on multiple generations of white micas (Lanterman Range, Antarctica), Earth Planet. Sci. Lett. 192 (2001) 389–405.
[16] E. Hagen, S.P. Kelley, H. Dypvik, O. Nilsen, B. Kjolhamar, Direct dating of authigenic K-feldspar overgrowths from the Kilombero Rift of Tanzania, J. Geol. Soc. 158 (2001) 801–807.
[17] S.P. Kelley, J.A. Wartho, Rapid kimberlite ascent and the significance of Ar-Ar ages in xenolith phlogopites, Science 289 (2000) 609–611.
[18] J.A. Wartho, S.P. Kelley, S. Blake, Magma flow regimes in sills deduced from Ar isotope systematics of host rocks, J. Geophys. Res. Solid Earth 106 (2001) 4017–4035.
[19] S.P. Kelley, J.M. Bartlett, N.B.W. Harris, Pre-metamorphic Ar-Ar ages from biotite inclusions in garnet, Geochim. Cosmochim. Acta 61 (1997) 3873–3878.
[20] L.J. Gaber, K.A. Foland, C.E. Corbato, On the significance of argon release from biotite and amphibole during 40Ar/39Ar vacuum heating, Geochim. Cosmochim. Acta 52 (1988) 2457–2465.
[21] J.K.W. Lee, T.C. Onstott, K.V. Cashman, R.J. Cumbest, D. Johnson, Incremental heating of hornblende in vacuo – Implications for Ar-40/Ar-39 geochronology and the interpretation of thermal histories, Geology 19 (1991) 872–876.
[22] V.W. Sletten, T.C. Onstott, The effect of the instability of muscovite during in vacuo heating on Ar-40/Ar-39 step-heating spectra, Geochim. Cosmochim. Acta 62 (1998) 123–141.
[23] I.M. Villa, J. Hermann, O. Müntener, V. Trommsdorff, Ar-39-Ar-40 dating of multiply zoned amphibole generations (Malenco, Italian Alps), Contrib. Mineral. Petrol. 140 (2000) 363–381.
[24] W. Müller, S.P. Kelley, I.M. Villa, Dating fault-generated pseudotachylytes: comparison of 40Ar/39Ar stepwise-heating, laser-ablation and Rb-Sr-microsampling analyses, Contrib. Mineral. Petrol. 144 (2002) 57–77.
[25] I.M. Villa, Radiogenic isotopes in fluid inclusions, Lithos 55 (2001) 115–124.
[26] T.C. Onstott, M.L. Miller, R.C. Ewing, G.W. Arnold, D.S. Walsh, Recoil refinements – Implications for the Ar-40/Ar-39 dating technique, Geochim. Cosmochim. Acta 59 (1995) 1821–1834.
[27] T.C. Onstott, C. Mueller, P.J. Vrolijk, D.R. Pevear, Laser Ar-40/Ar-39 microprobe analyses of fine-grained illite, Geochim. Cosmochim. Acta 61 (1997) 3851–3861.
[28] K.A. Foland, F.A. Hubacher, G.B. Arehart, Ar-40/Ar-39 dating of very fine-grained samples – an encapsulated-vial procedure to overcome the problem of Ar-39 recoil loss, Chem. Geol. 102 (1992) 269–276.

[29] B.A. van der Pluijm, C.M. Hall, P.J. Vrolijk, D.R. Pevear, M.C. Covey, The dating of shallow faults in the Earth's crust, Nature 412 (2001) 172–175.
[30] H.L. Dong, C.M. Hall, A.N. Halliday, D.R. Peacor, Laser Ar-40-Ar-39 dating of microgram-size illite samples and implications for thin section dating, Geochim. Cosmochim. Acta 61 (1997) 3803–3808.
[31] H.L. Dong, C.M. Hall, D.R. Peacor, A.N. Halliday, Mechanisms of argon retention in clays revealed by laser Ar-40-Ar-39 dating, Science 267 (1995) 355–359.
[32] S. Kelley, Excess argon in K-Ar and Ar-Ar geochronology, Chem. Geol. 188 (2002) 1–22.
[33] N.O. Arnaud, S.P. Kelley, Evidence for excess argon during high-pressure metamorphism in the Dora-Maira Massif (Western Alps, Italy), using an ultra-violet laser-ablation microprobe Ar-40-Ar-39 technique, Contrib. Mineral. Petrol. 121 (1995) 1–11.
[34] R.J. Cumbest, E.L. Johnson, T.C. Onstott, Argon composition of metamorphic fluids – Implications for Ar-40 Ar-39 geochronology, Geol. Soc. Am. Bull. 106 (1994) 942–951.
[35] S.C. Sherlock, N.O. Arnaud, Flat plateau and impossible isochrons: apparent Ar-40-Ar-39 geochronology in a high-pressure terrain, Geochim. Cosmochim. Acta 63 (1999) 2835–2838.
[36] H. Fritz, Kinematics and geochronology of Early Cretaceous thrusting in the northwestern Paleozoic of Graz (Eastern Alps), Geodin. Acta 2 (1988) 53–62.
[37] O. Hahn, F. Straßmann, J. Mattauch, H. Ewald, Geologische Altersbestimmungen nach der Strontiummethode, Chem.-Ztg. 67 (1943) 55–56.
[38] R.A. Cliff, Rb-Sr dating of white mica – new potential in metamorphic geochronology, Abstr. ICOG 8, US Geol. Surv. Circ. 1107 (1994) 62.
[39] W. Müller, N.S. Mancktelow, M. Meier, Rb-Sr microchrons of synkinematic mica in mylonites an example from the DAV fault of the Eastern Alps, Earth Planet. Sci. Lett. 180 (2000) 385–397.
[40] J.L. Birck, Precision K-Rb-Sr isotopic analysis: application to Rb-Sr chronology, Chem. Geol. 56 (1986) 73–83.
[41] S.H. Sie, T.R. Niklaus, G.F. Suter, Microbeam AMS: prospects of new geological applications, Nucl. Instrum. Methods Phys. Res. Sect. B Beam Interact. Mater. Atoms 123 (1997) 112–121.
[42] L.J. Moens, F.F. Vanhaecke, D.R. Bandura, V.I. Baranov, S.D. Tanner, Elimination of isobaric interferences in ICP-MS, using ion-molecule reaction chemistry: Rb/Sr age determination of magmatic rocks, a case study, J. Anal. At. Spectrom. 16 (2001) 991–994.
[43] J.N. Christensen, A.N. Halliday, D.C. Lee, C.M. Hall, In-situ Sr isotopic analysis by laser-ablation, Earth Planet. Sci. Lett. 136 (1995) 79–85.
[44] J. Davidson, F. Tepley III, Z. Palacz, S. Meffan-Main, Magma recharge, contamination and residence times revealed by in situ laser ablation isotopic analysis of feldspar in volcanic rocks, Earth Planet. Sci. Lett. 184 (2001) 427–442.
[45] S. Meffan-Main, Cliff, R.A., Strontium isotope exchange on a sub-millimetre scale and the implications for rubidium-strontium dating of basement gneisses, Seventh Annual V.M. Goldschmidt Conference, LPI Contrib. 921 (1997) 139–140.
[46] M. Frey, J.C. Hunziker, J.R. O'Neil, H.W. Schwander, Equilibrium-disequilibrium relations in the Monte Rosa granite, Western Alps: petrological, Rb-Sr and stable isotope data, Contrib. Mineral. Petrol. 55 (1976) 147–179.
[47] F. Begemann, K.R. Ludwig, G.W. Lugmair, K. Min, L.E. Nyquist, P.J. Patchett, P.R. Renne, C.Y. Shih, I.M. Villa, R.J. Walker, Call for an improved set of decay constants for geochronological use, Geochim. Cosmochim. Acta 65 (2001) 111–121.
[48] E. Scherer, C. Münker, K. Mezger, Calibration of the lutetium-hafnium clock, Science 293 (2001) 683–687.
[49] E.E. Scherer, K.L. Cameron, J. Blichert-Toft, Lu-Hf garnet geochronology: closure temperature relative to the Sm-Nd system and the effects of trace mineral inclusions, Geochim. Cosmochim. Acta 64 (2000) 3413–3432.
[50] J. Ganguly, M. Tirone, R.L. Hervig, Diffusion kinetics of samarium and neodymium in garnet, and a method for determining cooling rates of rocks, Science 281 (1998) 805–807.
[51] S. Duchene, J. Blichert-Toft, B. Luais, P. Telouk, J.M. Lardeaux, F. Albarede, The Lu-Hf dating of garnets and the ages of the Alpine high- pressure metamorphism, Nature 387 (1997) 586–589.
[52] C.I. Prince, J. Kosler, D. Vance, D. Günther, Comparison of laser ablation ICP-MS and isotope dilution REE analyses – implications for Sm-Nd garnet geochronology, Chem. Geol. 168 (2000) 255–274.
[53] D. Vance, N. Harris, Timing of prograde metamorphism in the Zanskar Himalaya, Geology 27 (1999) 395–398.
[54] C.P. DeWolf, C.J. Zeissler, A.N. Halliday, K. Mezger, E.J. Essene, The role of inclusions in U-Pb and Sm-Nd garnet geochronology: stepwise dissolution experiments and trace uranium mapping by fission track analysis, Geochim. Cosmochim. Acta 60 (1996) 121–134.
[55] D. Vance, M. Meier, F. Oberli, The influence of high U-Th inclusions on the U-Th-Pb systematics of almandine-pyrope garnet: results of a combined bulk dissolution, stepwise-leaching, and SEM study, Geochim. Cosmochim. Acta 62 (1998) 3527–3540.
[56] M. Thöni, E. Jagoutz, Some new aspects of dating eclogites in orogenic belts – Sm-Nd, Rb-Sr, and Pb-Pb isotopic results from the Austroalpine Saualpe and Koralpe type-locality (Carinthia/Styria, Southeastern Austria), Geochim. Cosmochim. Acta 56 (1992) 347–368.
[57] B. Luais, S. Duchene, J. deSigoyer, Sm-Nd disequilibrium in high-pressure, low-temperature Himalayan and Alpine rocks, Tectonophysics 342 (2001) 1–22.
[58] Y.-F. Zheng, Z.-R. Wang, S.-G. Li, Z.-F. Zhao, Oxygen isotope equilibrium between eclogite minerals and its constraints on mineral Sm-Nd chronometer, Geochim. Cosmochim. Acta 66 (2002) 625–634.
[59] C.P. DeWolf, N. Belshaw, R.K. O'Nions, A Metamor-

phic history from micron-scale Pb-207/Pb-206 chronometry of Archean Monazite, Earth Planet. Sci. Lett. 120 (1993) 207–220.
[60] G. Foster, P. Kinny, D. Vance, C. Prince, N. Harris, The significance of monazite U-Th-Pb age data in metamorphic assemblages; a combined study of monazite and garnet chronometry, Earth Planet. Sci. Lett. 181 (2000) 327–340.
[61] M. Grove, T.M. Harrison, Monazite Th-Pb age depth profiling, Geology 27 (1999) 487–490.
[62] K. Viskupic, K.V. Hodges, Monazite-xenotime thermochronometry: methodology and an example from the Nepalese Himalaya, Contrib. Mineral. Petrol. 141 (2001) 233–247.
[63] J.M. Pyle, F.S. Spear, R.L. Rudnick, W.F. McDonough, Monazite-xenotime-garnet equilibrium in metapelites and a new monazite-garnet thermometer, J. Petrol. 42 (2001) 2083–2107.
[64] G. Andrehs, W. Heinrich, Experimental determination of REE distributions between monazite and xenotime: potential for temperature-calibrated geochronology, Chem. Geol. 149 (1998) 83–96.
[65] D.P. Hawkins, S.A. Bowring, U-Pb systematics of monazite and xenotime: case studies from the Paleoproterozoic of the Grand Canyon, Arizona, Contrib. Mineral. Petrol. 127 (1997) 87–103.
[66] D. Rubatto, D. Gebauer, Use of cathodoluminescence for U-Pb zircon dating by ion microprobe: some examples from the Western Alps, in: M. Pagel, V. Barbin, P. Blanc, D. Ohnenstetter (Eds.), Cathodoluminescence in Geosciences, Springer, Berlin, 2000, pp. 373–400.
[67] A. Liati, D. Gebauer, Constraining the prograde and retrograde P-T-t path of Eocene HP rocks by SHRIMP dating of different zircon domains: inferred rates of heating, burial, cooling and exhumation for central Rhodope, northern Greece, Contrib. Mineral. Petrol. 135 (1999) 340–354.
[68] D. Rubatto, J. Hermann, Exhumation as fast as subduction?, Geology 29 (2001) 3–6.
[69] J. Hermann, D. Rubatto, A. Korsakov, V.S. Shatsky, Multiple zircon growth during fast exhumation of diamondiferous, deeply subducted continental crust (Kokchetav Massif, Kazakhstan), Contrib. Mineral. Petrol. 141 (2001) 66–82.
[70] G. Fraser, D. Ellis, S. Eggins, Zirconium abundance in granulite-facies minerals, with implications for zircon geochronology in high-grade rocks, Geology 25 (1997) 607–610.
[71] D. Rubatto, Zircon trace element geochemistry: partitioning with garnet and the link between U-Pb ages and metamorphism, Chem. Geol. 184 (2002) 123–138.
[72] I. Horn, R.L. Rudnick, W.F. McDonough, Precise elemental and isotope ratio determination by simultaneous solution nebulization and laser ablation-ICP-MS: application to U-Pb geochronology, Chem. Geol. 164 (2000) 281–301.
[73] J.R. Ballard, J.M. Palin, I.S. Williams, I.H. Campbell, A. Faunes, Two ages of porphyry intrusion resolved for the super-giant Chuquicamata copper deposit of northern Chile by ELA-ICP-MS and SHRIMP, Geology 29 (2001) 383–386.
[74] W. Compston, Geological age by instrumental analysis: the 29th Hallimond Lecture, Mineral. Mag. 63 (1999) 297–311.
[75] R.H. Steiger, R.A. Bickel, M. Meier, Conventional U-Pb dating of single fragments of zircon for petrogenetic studies of phanerozoic granitoids, Earth Planet. Sci. Lett. 115 (1993) 197–209.
[76] F. Oberli, M. Meier, A. Berger, C. Rosenberg, r. Giere, U-Th-Pb and 230Th/238U disequilibrium isotope systematics: precise accessory mineral chronology and melt evolution tracing in the Alpine Bergell intrusion, Geochim. Cosmochim. Acta (2002) in press.
[77] S. Bodorkos, P.A. Cawood, N.H.S. Oliver, Timing and duration of syn-magmatic deformation in the Mabel Downs Tonalite, northern Australia, J. Struct. Geol. 22 (2000) 1181–1198.
[78] D.A. Richards, S.H. Bottrell, R.A. Cliff, K. Strohle, P.J. Rowe, U-Pb dating of a speleothem of Quaternary age, Geochim. Cosmochim. Acta 62 (1998) 3683–3688.
[79] E.T. Rasbury, G.N. Hanson, W.J. Meyers, A.H. Saller, Dating of the time of sedimentation using U-Pb ages for paleosol calcite, Geochim. Cosmochim. Acta 61 (1997) 1525–1529.
[80] N.C. Sturchio, M.R. Antonio, L. Saderholm, S.R. Sutton, J.C. Brannon, Tetravalent uranium in calcite, Science 281 (1998) 971–973.
[81] J.G. Ramsay, M.I. Huber, The Techniques of Modern Structural Geology, Vol. 1. Strain Analysis, Academic Press, London, 1983, 687 pp.
[82] D. Aerden, The pyrite-type strain fringes from Lourdes (France): indicators of Alpine thrust kinematics in the Pyrenees, J. Struct. Geol. 18 (1996) 75–91.
[83] D. Vance, E. Mahar, Pressure-temperature paths from P-T pseudosections and zoned garnets: potential, limitations and examples from the Zanskar Himalaya, NW India, Contrib. Mineral. Petrol. 132 (1998) 225–245.
[84] S.H. Sie, D.A. Sims, T.R. Niklaus, F. Bruhn, G. Suter, G. Cripps, In situ microanalysis for trace element and isotopic data by AMS, Nucl. Instrum. Methods Phys. Res. Sect. B Beam Interact. Mater. At. 158 (1999) 201–208.
[85] I.M. Villa, Isotopic closure, Terra Nova 10 (1998) 42–47.
[86] H. Peresson, K. Decker, The Tertiary dynamics of the northern Eastern Alps (Austria): changing palaeostresses in a collisional plate boundary, Tectonophysics 272 (1997) 125–157.
[87] S.M. Eggins, L.P.J. Kinsley, J.M.G. Shelley, Deposition and element fractionation processes during atmospheric pressure laser sampling for analysis by ICP-MS, Appl. Surf. Sci. 129 (1998) 278–286.
[88] J.C. Brannon, S.C. Cole, F.A. Podosek, V.M. Ragan, R.M. Coveney, M.W. Wallace, A.J. Bradley, Th-Pb and U-Pb dating of ore-stage calcite and Paleozoic fluid flow, Science 271 (1996) 491–493.

[89] W. Müller, R.D. Dallmeyer, F. Neubauer, M. Thöni, Deformation-induced resetting of Rb/Sr and Ar-40/Ar-39 mineral systems in a low-grade, polymetamorphic terrane (Eastern Alps, Austria), J. Geol. Soc. 156 (1999) 261–278.
[90] T.W. Argles, C.I. Prince, G.L. Foster, D. Vance, New garnets for old? Cautionary tales from young mountain belts, Earth Planet. Sci. Lett. 172 (1999) 301–309.
[91] D. Giorgis, M. Cosca, S.G. Li, Distribution and significance of extraneous argon in UHP eclogite (Sulu terrain, China): insight from in situ Ar-40/Ar-39 UV-laser ablation analysis, Earth Planet. Sci. Lett. 181 (2000) 605–615.
[92] R. Anczkiewicz, M. Thirlwall, J.P. Platt, Influence of inclusions and leaching techniques on Sm-Nd and Lu-Hf garnet chronology, Geochim. Cosmochim. Acta 66 (2002) A19 (abstr.).
[93] J.M. Amato, C.M. Johnson, L.P. Baumgartner, B.L. Beard, Rapid exhumation of the Zermatt-Saas ophiolite deduced from high-precision Sm-Nd and Rb-Sr geochronology, Earth Planet. Sci. Lett. 171 (1999) 425–438.

Wolfgang Müller (Ph.D., 1998, Swiss Federal Institute of Technology (ETH) Zürich) currently is Postdoctoral Fellow at the Research School of Earth Sciences, Australian National University, Canberra. He uses isotope geochemistry to tackle a wide range of problems in the earth sciences, archaeology and anthropology. During his Ph.D. and earliest postdoc period he improved techniques for dating deformation, in order to constrain rates and durations of activity in fault zones. Currently, he uses radiogenic and stable isotopic tracers in biominerals to reconstruct human origin and migration, and works towards an improved U–Th–Pa disequilibrium chronology for the later stages of human evolution.